CoA NOTE MAT. No. 25

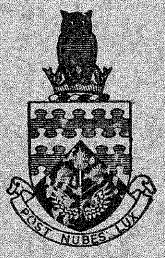

THE COLLEGE OF AERONAUTICS
CRANFIELD

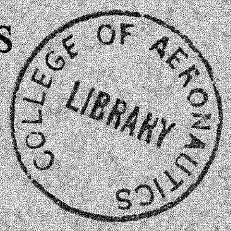

A FRACTURE OF RUBBER IN A STATE OF FINITE TORSIONAL SHEAR

by

M. M. Hall and A. R. Sollars

CoA Note Mat. No. 25

January, 1969

THE COLLEGE OF AERONAUTICS

DEPARTMENT OF MATERIALS

A fracture of rubber in a state of finite torsional shear

- by -

M.M. Hall, B.Sc., Ph.D., A.Inst.P.

and

A.R. Sollars, B.Sc.

ABSTRACT

A solid rubber cylinder with metal end plates fractured in the rubber when a torsional deformation was applied which corresponded to a shear angle of 56° on the cylinder surface. The height of the cylinder was maintained accurately constant during the deformation. A comparatively smooth fracture surface was created in a direction perpendicular to the principal tensile stress and a rough surface was created perpendicular to the principal compressive stress. The markings on the smooth surface have some feature similar to a cleavage-type failure in a crystalline material.

Contents

1. Introduction

An interesting mode of failure has been observed in a solid rubber cylinder which had metal end plates bonded onto the flat ends. The failure occurred during studies of the stress distribution necessary to maintain the rubber in a state of finite torsional shear.

It has been shown (Rivlin, 1956) that the surface tractions necessary to maintain a right circular cylinder in a state of finite torsional shear correspond to two sets of stress components each acting only over the plane ends of the cylinder. In addition to the distribution of tangential surface tractions providing the twisting couple, a distribution of normal surface tractions is required to maintain the cylinder at constant length. In the work described in this Note the torsional shear was maintained by mounting the rubber unit vertically in such a manner as to allow the bottom plate to be twisted with respect to the top plate, while maintaining the length constant to an accuracy of better than 0.05% (Hall, 1968).

Fracture was observed in a particular rubber when one end of the unit was twisted through 25° with respect to the other end. The failure was unintentional. Two distinct types of fracture surfaces were created and the nature of these surfaces has been studied. The directions of the fracture path have been examined in terms of the stress distribution through the rubber.

A limited number of attempts were made to reproduce the complete mode of failure by deliberately initiating a fracture in other specimens of rubber in a similar state of shear. Only one type of fracture surface was created, the nature and direction corresponding to the relatively smooth primary fracture surfaces discussed in sections 2 and 3.

The rubber was an unfilled natural rubber, vulcanised for 30 minutes at 150°C using 5% by weight of dicumyl peroxide. The rubber cylinder was 4 inches in diameter and 0.57 inches long.

2. The directions of the fracture path on the cylinder surface

The shear strain at the curved surface of the rubber cylinder was about 150%, (i.e. a shear angle of about 56°) when failure occurred. The deformation was then removed. The fracture path on the curved surface of the undeformed rubber can be seen in figure 1(a) and also in the diagram of the fracture (figure 1(b)). The deformation had been imposed by twisting the bottom plate DD^1 from left to right with respect to the top plate A^1A.

The fracture was clearly initiated at A. The short line AB is at 45° to the direction of twist and therefore in the deformed state AB was perpendicular to the principal tensile stress. This is the direction the initial part of a fracture path would be expected to follow. The initial part of the fracture CF is perpendicular to AD at C.

In attempting to understand the nature of the fracture it is necessary to consider the directions of the fracture path in the deformed rubber. These directions are shown in figure 2, together with the principal stress directions at the instant before failure. Details of the methods of calculation of the relevant angles are given in Appendix A.

A possible order in which the complete fracture was generated is as follows. Consider figure 2(b). The crack was initiated at A, in a direction AB^1 perpendicular to the maximum tensile stress and the direction then changed to B^1X^1. The abrupt change in direction presumably occurred at a flaw. The newly created surfaces along B^1X^1 are rough which suggests that this part of the fracture was at a rate of propagation slow enough to allow rubber to behave as an elastomer rather than as a glass-like brittle material. The crack then propagated rapidly along X^1D^1, creating comparatively smooth glass-like surfaces.

It is probable from considerations of the Griffith fracture criterion in three dimensions, that X^1D^1 is perpendicular to the new principal tensile stress direction after local stress redistribution at the crack tip. The Griffith criterion for a critical fracture stress in a uniaxial stress system has been extended to two and three dimensional systems by a number of workers and discussed by Andrews (1968). He reports that if the principal stresses σ_1 and σ_2 are such that $3\sigma_1 + \sigma_2 > 0$, then the most favoured direction for crack propagation is perpendicular to the principal tensile stress σ_1. We will now show that the criteria $3\sigma_1 + \sigma_2 > 0$ is obeyed for a solid rubber cylinder in a state of finite torsional shear.

If we assume that W, the elastic free energy which is stored in the rubber during deformation, can be described by the kinetic theory of rubber-like elasticity then,

$$W = C_1(I_1-3) \tag{2.1}$$

where C_1 is a material parameter related to the shear modulus of the rubber, and I_1 is a strain invariant. (Treloar, 1958). The strain matrix σ_{ij} for finite simple shear in an incompressible material has been derived by Rivlin, (Rivlin, 1956) for a completely general form of W. If W is given by (2.1), then it can be shown that σ_{ij} is given by

$$(\sigma_{ij}) = \begin{pmatrix} 2\psi^2 r^2 C_1 & 2\psi r C_1 & 0 \\ 2\psi r C_1 & 0 & 0 \\ 0 & 0 & 1 \end{pmatrix} \tag{2.2}$$

$(i,j = 1,2, \text{ or } 3)$

where r is the radial displacement from the cylinder axis and ψ is the angular twist per unit length. The local coordinate axes Ox_1 and Ox_2 are in the directions tangential to the curved cylinder surface, and in the direction of the cylinder axis respectively.

If the axes are rotated by an angle α about the Ox_3 axis, (the radial direction) then it can be shown that the transformed stress matrix (σ_{ij}^{1}) is given by

$$(\sigma_{ij}^{1}) = \begin{pmatrix} 2\psi rC_1 \sin 2\alpha + 2\psi^2 r^2 C_1 \cos 2\alpha & 2\psi rC_1 \cos 2\alpha - \psi^2 r^2 C_1 \sin 2\alpha \\ 2\psi rC_1 \cos 2\alpha - \psi^2 r^2 C_1 \sin 2\alpha & 2\psi^2 r^2 C_1 \sin 2\alpha - 2\psi rC_1 \sin 2\alpha \end{pmatrix} \qquad (2.3)$$

$(i,j = 1 \text{ or } 2)$

Hence

$$3\sigma_{11}' + \sigma_{22}' = 4\psi rC_1 \sin 2\alpha + 4\psi^2 r^2 C_1 \cos 2\alpha + 2\psi^2 r^2 C_1 \qquad (2.4)$$

If the new axis directions coincided with the direction of the principal axes, then

$$\sigma_{11}' = \sigma_1 \text{ and } \sigma_{22}' = \sigma_2$$

Now, from 2.3, (or Appendix A(ii)) the direction of the principal axes on the surface of the cylinder is given by the value of the angle α when the shear stress components in the stress matrix σ_{ij}' are zero.

i.e. when $\tan 2\alpha = \dfrac{2}{\psi a}$ (2.5)

where a is the radius of the cylinder. Therefore at a surface shear strain of 150% ($\psi a = 1.5$), substitution of (2.5) into (2.4) shows that $\sigma_1 + 3\sigma_2 > 0$.

Examination of the fractured rubber cylinder showed that the fracture surfaces bounded by X^1D^1 only penetrated about a quarter of the way in towards the axis of the cylinder. The bulk of the cylinder therefore remained stressed after the creation of these surfaces. It is therefore likely that the crack X^1D^1 was opened out by these residual stresses because the cylinder remained in its twisted state. The stress system in the new surface then included a tensile stress component which would be a maximum at the cylinder surface, presumably at C which is midway between the end plates. A second crack then propagated. CE, the first part of the edge of the secondary crack, is perpendicular to the primary fracture. The roughness of the new surfaces along CEF suggested considerable stress-reorientation as the fracture propagated as a consequence of a comparatively low rate of propagation.

3. The fracture surface markings

The major surface markings on the undeformed fracture faces bounded by the edge AD (see figure 1) are clearly shown in figures 5(a) and 5(b). These matching surfaces can be identified with figure 1 by noting the secondary fracture surface edge in figure 5(b).

Examination of these surfaces revealed two distinct sets of markings. The major curved markings are clearly visible in figures 5(a) and 5(b) and are shown diagrammatically in figure 6(b). In addition, finer markings could be discerned which appeared to be something like 30° to these major markings. Due to the low reflectivity of the fracture surfaces however, photography of these fine markings was extremely difficult and therefore a gelatine replica of the surface was prepared, using a 25% solution of gelatine in water. A replica approximately 1/16" thick was produced, mechanically stripped from the surface shown in figure 5(a), lightly shadowed with platinum and then examined in transmitted light on a Vickers projection microscope.

These fine markings, referred to above, are shown clearly in figure 7, as fine cross markings. Figures 8,9 and 10 show further details of the fracture surface revealing elongated facets running in the direction of the major markings shown in figures 5(a) and 5(b). These three photographs refer to three well separated positions on the fracture surface and are typical of the whole fracture surface. At higher magnifications markings of the type shown in figures 11 and 12 were found.

Careful examination of all these markings indicates that they are, in fact, different aspects of the finer markings indicated in figure 7 and we believe that the fracture surface consists of small facets (e.g. figure 9) and fine steps. The general featureless appearance of the surface between steps indicates that the fracture has progressed in a manner reminiscent of a cleavage type failure.

Burghard and Stoloff (1968) in their paper on the fractography of cleavage failures have published a fractograph of a cleavage failure in a steel which is very similar to figures 9 and 10. They also state that facets of the type shown are generally associated with cleavage involving extensive local deformation.

It is well known that, at high deformations, natural rubber becomes partially crystalline (Treloar 1958). Therefore, a possible explanation of the observed fracture characteristics is that the localised high strain ahead of the progressing crack causes crystallisation and that failure is then through material which can undergo cleavage. It should be noted, however, that this places a restriction upon the crack propagation rate because of the time necessary to allow for the development of the local crystalline regions. The size of the facets on the rubber fracture are larger, by a factor of several hundreds, than those in the steel fractograph.

The secondary fracture face (CEF in figure 1(b)) shows quite different characteristics (figure 13). The surface is generally rough and no features of the type discussed above are to be seen and it appears to be a typical tearing fracture face.

4. Summary

The directions of the fracture paths on the surface of the deformed rubber cylinder coincide with the directions adopted by the principal stresses. Failure in torsion by a crack propagating perpendicular to the maximum tensile stress is well known for many materials, but biaxial failure in torsion has not, within the knowledge of the authors, been previously reported. It is possible however that the presence of the secondary tear type of crack is fortuitous. Having started at a flaw at F (Figure 2) and propagating towards C, within the time scale of the propagation of X^1D^1.

References

1. Hall, M.M. — College of Aeronautics Note Mat. No. 17, 1968.

2. Rivlin, R.S. — Rheologs Volume 1 (ed. Eirich), Academic Press, 1956.

3. Treloar, L.R.G. — The Physics of Rubber Elasticity 2nd. ed. (Clarendon Press) 1958.

4. Burghard, H.C. and Stoloff, N.S. — Electron Fractography, A.S.T.M. S.T.P.436 1968, pp. 32-58.

Appendix A

(i) To calculate the direction of the fracture paths in the deformed rubber. The cylinder of radius a and length ℓ has one end twisted through θ radians.

In the undeformed state the fracture AD makes an angle of 28° with the bottom plate (figure 3). If AD takes up the position AD^1 in the deformed state, then $DD^1 = a\theta$ and the angular direction of AD^1 is given by:

$$\frac{\ell}{\sin 28 \sin\beta} = \frac{a\theta}{\sin(152-\beta)} \qquad (A.1)$$

(A.1) is derived simply by using the sine rule for the triangle ADD^1.

Now a = 2.0 inches

ℓ = 0.57 inches

θ = 25° = 0.436 radians.

Hence β = 109°

Consider now CE, the part of the fracture CF which is perpendicular to AD in the undeformed state. Suppose it adopts the position C^1E^1 in the deformed state. C and C^1 are midway between the Z end plates.

Let E have the coordinate x and y w.r.t. the axes CC^1 and Co which intersect at the origin C.

Hence γ, the angular direction of the crack in the deformed state, is given by:

$$\tan\gamma = \frac{C^1P}{PE^1} = \frac{y}{PE^1} \qquad (A.2)$$

where

$$PE^1 = EE^1 + x - CC^1 \qquad (A.3)$$

Now

$$CC^1 = \frac{a\theta}{2} \qquad (A.4)$$

and

$$EE^1 \text{ is given by } \frac{EE^1}{a\theta} = \frac{y+\ell/2}{\ell} \qquad (A.5)$$

Hence by substituting (A.3), (A.4) and (A.5) into (A.2)

$$\tan\gamma = \frac{\ell y}{\ell x + a\theta y} \qquad (A.6)$$

The measured values of x and y are x = 0.024 inches, y = 0.046 inches. Hence $\gamma = 26°$

(ii) The principal stress directions on the curved surface of the cylinder

The direction of the principal axes are the directions of the semi-major and semi-minor axes of the strain ellipse PQRS. (figure 4). In the undeformed state the ellipse was the circle $P^1Q^1R^1S^1$ of radius $\ell/2$. If the length of the major axis is $\ell\lambda$, then the length of the minor axes is ℓ/λ since shear is a constant volume deformation.

The shear angle ϕ is given by

$$\tan\phi = \frac{a\theta}{\ell}$$

Let Ox and Oy be rectangular coordinate axes fixed in space. The principal stress axes make an angle α with Ox as shown. Let axes Ox^1 and Oy^1 lie in the direction of the major and minor axes respectively.

If (x^1,y^1) is a point on the ellipse, w.r.t. Ox^1 and Oy^1, then the equation of the ellipse is

$$\frac{(x^1)^2}{\lambda^2} + \lambda^2(y^1)^2 = \frac{\ell^2}{4}$$

It can be shown that if the point (x^1,y^1) has coordinates (x,y) w.r.t. Ox and Oy, then

$$x^1 = x\cos\alpha + y\sin\alpha$$
$$y^1 = x\sin\alpha + y\cos\alpha \qquad (A.9)$$

and therefore the equation of the ellipse w.r.t. Ox and Oy is

$$\frac{(x\cos\alpha - y\sin\alpha)^2}{\lambda^2} + \lambda^2(x\sin\alpha + y\cos\alpha)^2 = \frac{\ell^2}{4} \qquad (A.10)$$

Now the point Q with coordinates $x = \ell/2$, $y = 0$, lies on the ellipse, and hence by substitution into (A.10)

$$\lambda = \cot\alpha \qquad (A.11)$$

Similarly substituting the point R, $x = \frac{\ell}{2}\tan\phi$, $y = -\frac{\ell}{2}$, into (A.10), and using (A.7) and (A.11), then

$$\tan 2\alpha = \frac{2\ell}{a\theta} \qquad (A.12)$$

and hence $\alpha = 26°$.

Appendix B

To find the position of the fracture surface markings when the rubber was in the deformed state.

The surface markings on the undeformed fracture surface which have an edge AD (figure 1) are shown in figure 6(a). Consider a series of n points, (X_i say, where i has the values 1,2,3, ..., n), which lie along any one of the major markings. The positions X_i' of these markings when the rubber cylinder was deformed give the position of that particular surface marking in the deformed state.

The radial displacement of X_i from the axis of the rubber cylinder, and the vertical position between the end plates will be invariant as the cylinder is twisted.

Consider a surface concentric with the curved surface of the cylinder and at a radial distance r (< a) from the axis (figure 6(b)). Let X be at a distance h from the top plate where h is measured in the plane of the fracture surface. Let X^1, the position of X in the deformed state, be at a distance h^1 from the top plate. Then

$$h^1 = h \frac{\sin WYY^1}{\sin(180-WY^1Y)} \qquad (B.1)$$

If the angles WYY^1 and WY^1Y are known, then the position of X^1 for any known point X can be calculated from (B.1).

On the surface of the cylinder, angle $WYY^1 = 28°$ and angle $AY^1Y = 92°$, and hence from (B.1)

$$h^1 = 0.47h \qquad (B.2)$$

At a radial distance r = 0.8a the measured value of angle WYY^1 is about 35°, and hence from (A.1) angle WY^1Y is 98° and therefore

$$h^1 = 0.57h \qquad (B.3)$$

The transformed positions of the points X_1 and X_2 which lie on the same surface marking (figure 6(a)) have been calculated using (B.2) and (B.3). Hence $X_1^1X_2^1$ is the position adopted by the marking X_1X_2 when the rubber is in the deformed state.

The angle between the major markings and the second set of comparatively short broken markings is approximately 30° (see section 3) and is virtually unaltered during the removal of the torsional shear.

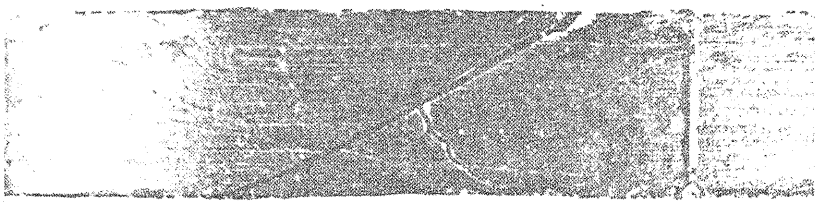

FIGURE 1. (a)
THE FRACTURE AT THE SURFACE OF THE UNDEFORMED RUBBER CYLINDER

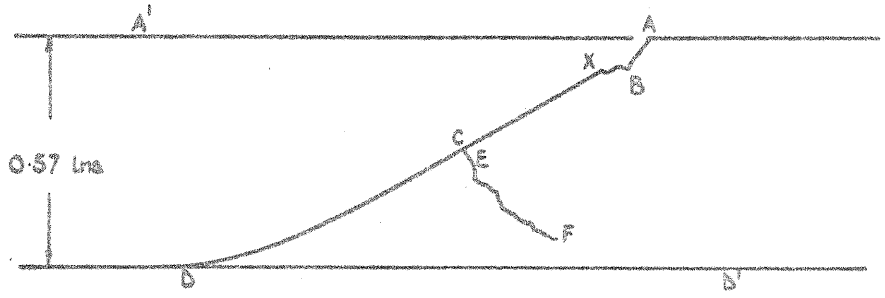

FIGURE 1(b)
A DIAGRAM OF THE FRACTURE SHOWN IN FIGURE 1(a).

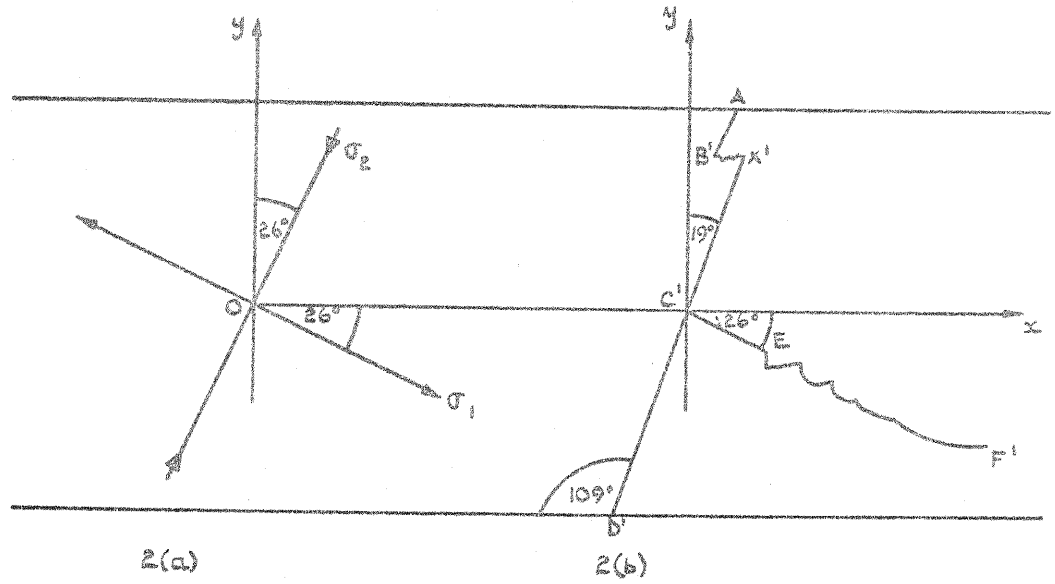

FIGURE 2.
(a) THE PRINCIPAL STRESS DIRECTIONS ON THE RUBBER SURFACE AT THE MOMENT BEFORE FRACTURE.
(b) THE POSITION OF THE CRACKS ON THE CURVED SURFACE WHEN THE RUBBER CYLINDER IS IN THE DEFORMED STATE.

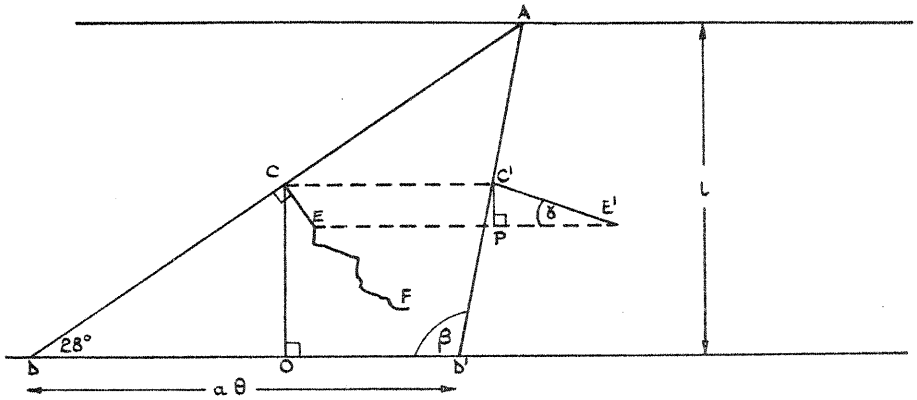

FIGURE. 3.
A DIAGRAM TO AID CALCULATION OF THE POSITION OF THE FRACTURE PATHS ON THE CURVED SURFACE OF THE DEFORMED RUBBER CYLINDER. (SEE APPENDIX A(i)).

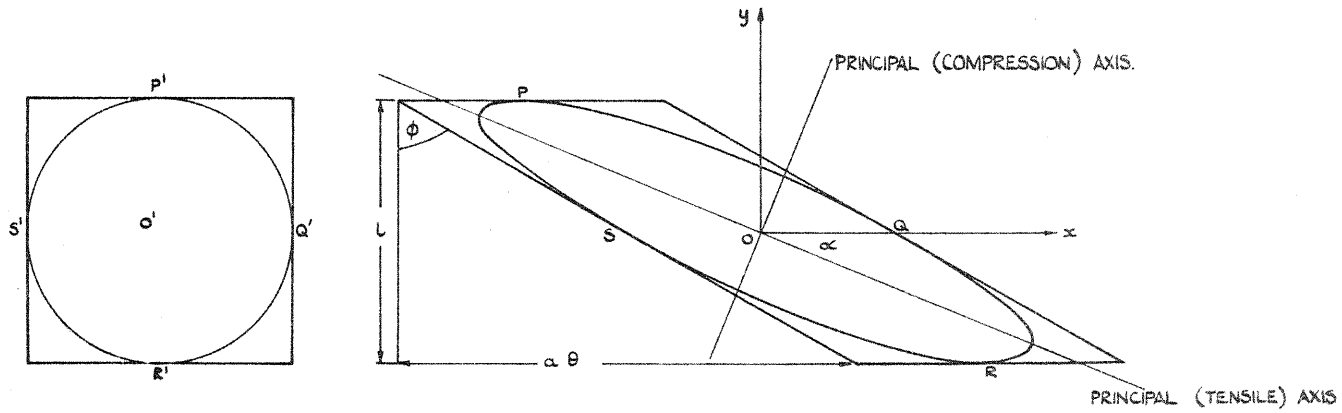

FIGURE 4.
A DIAGRAM TO AID CALCULATION OF THE PRINCIPAL STRESS DIRECTIONS ON THE CURVED SURFACE OF THE DEFORMED RUBBER CYLINDER. (SEE APPENDIX A (ii))

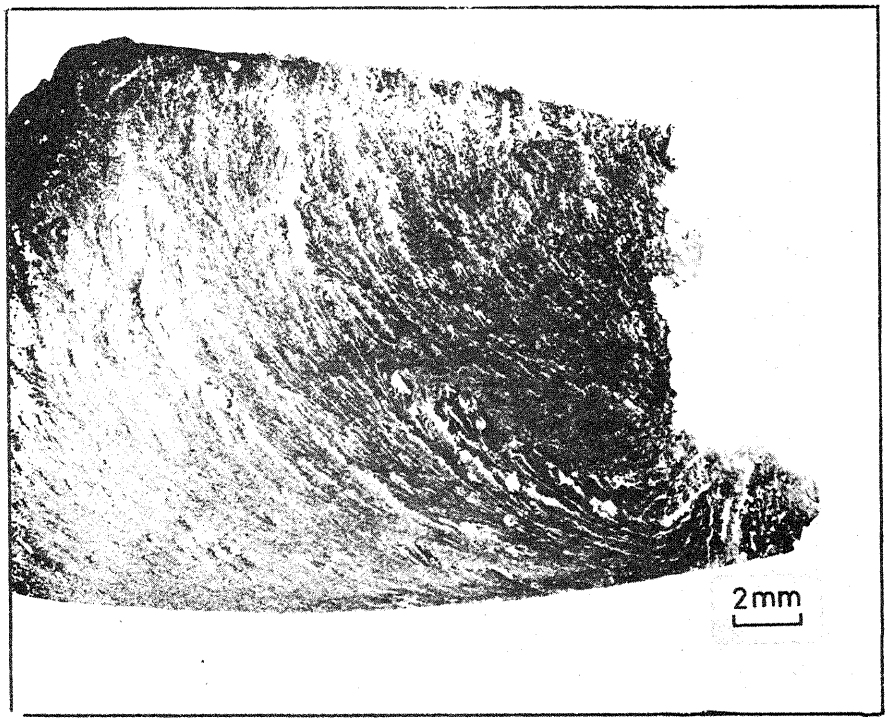

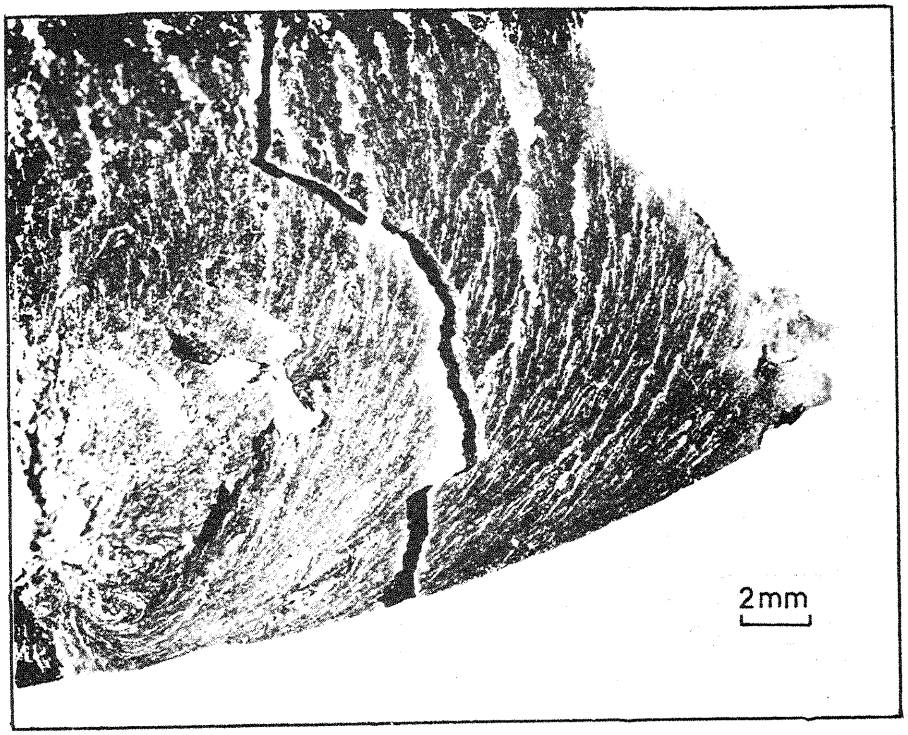

FIGURES 5(a), 5(b)
THE MATCHING FRACTURE SURFACES BOUNDED BY THE EDGE AD

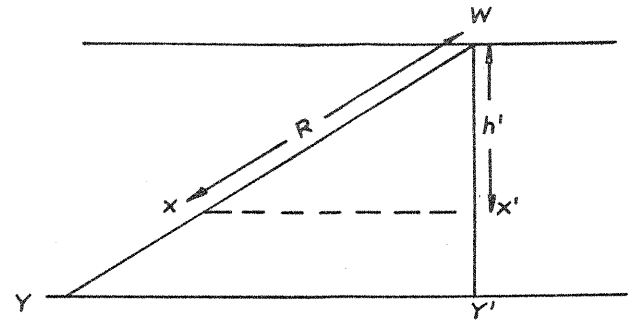

FIGURE 6(a)

THE CHANGE IN POSITION OF A POINT X ON THE FRACTURE SURFACE AD. THE AREA WYY' IS PART OF A SURFACE CONCENTRIC WITH THE CURVED SURFACE OF THE CYLINDER (SEE APPENDIX B).

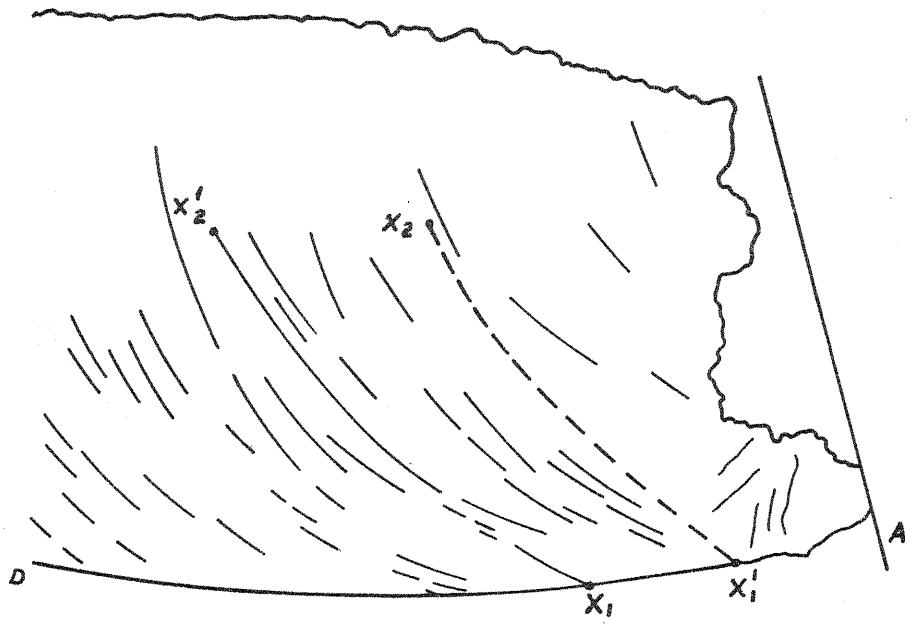

FIGURE 6 (b)

A DIAGRAM OF THE MARKING IN THE FRACTURE SURFACE BOUNDARY BY THE EDGE AD. (SEE FIGURES 1(b) AND 5(a)).

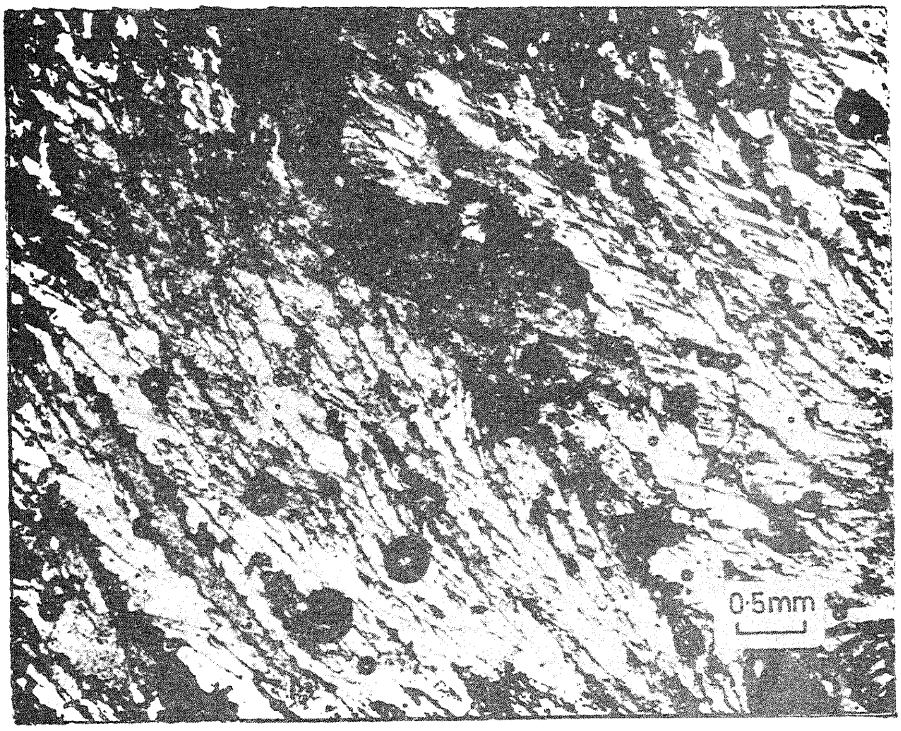

FIGURE 7
SECONDARY MARKINGS ON THE MAIN FRACTURE SURFACE

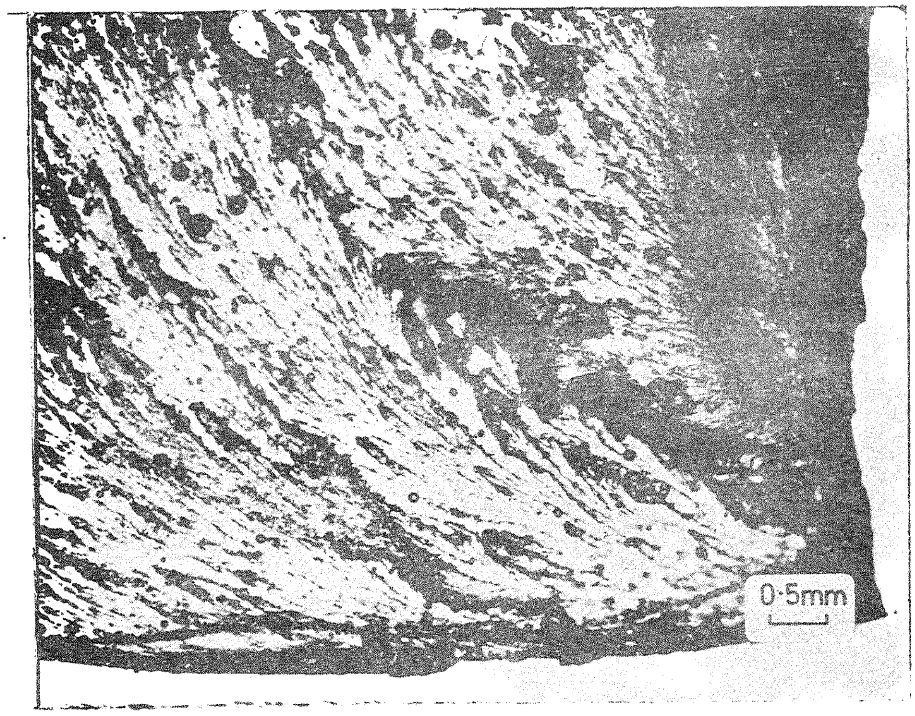

FIGURE 8
FACETS ON MAIN FRACTURE SURFACE

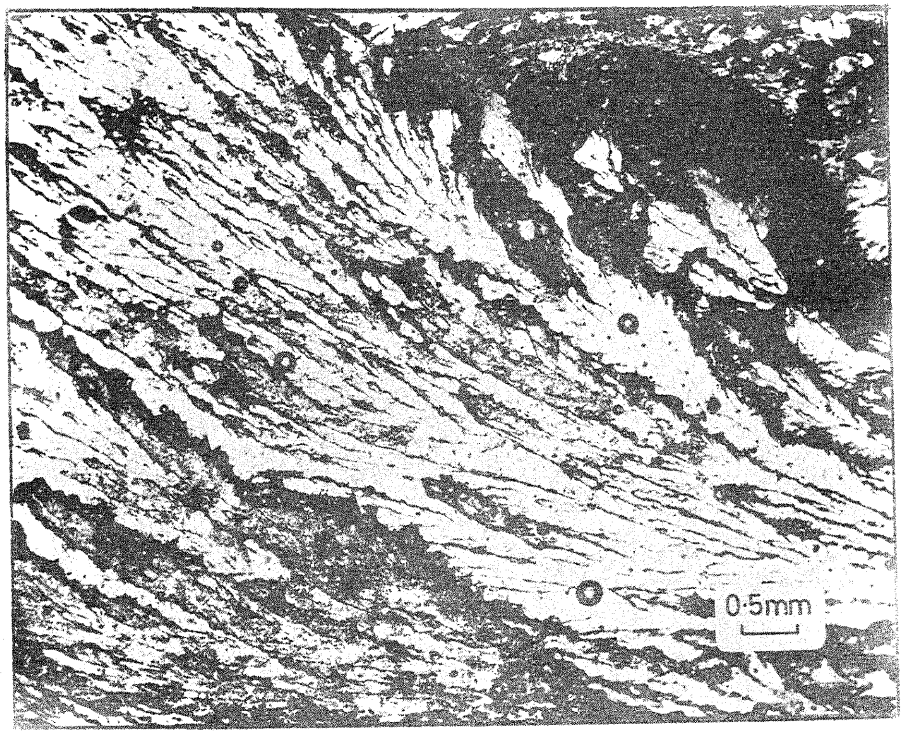

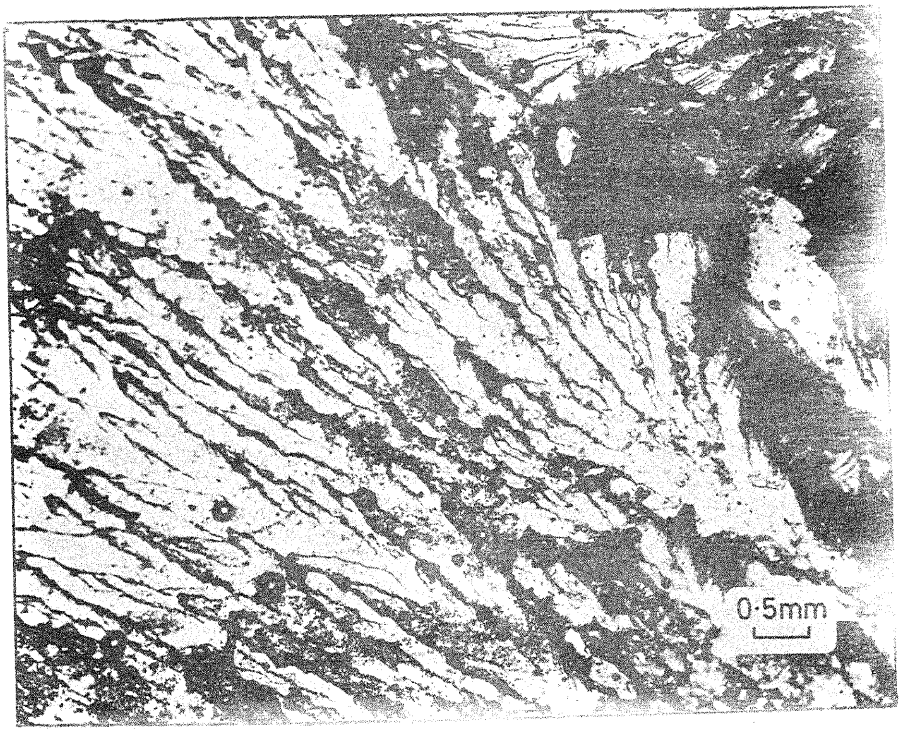

FIGURES 9, 10
FACETS ON MAIN FRACTURE SURFACE

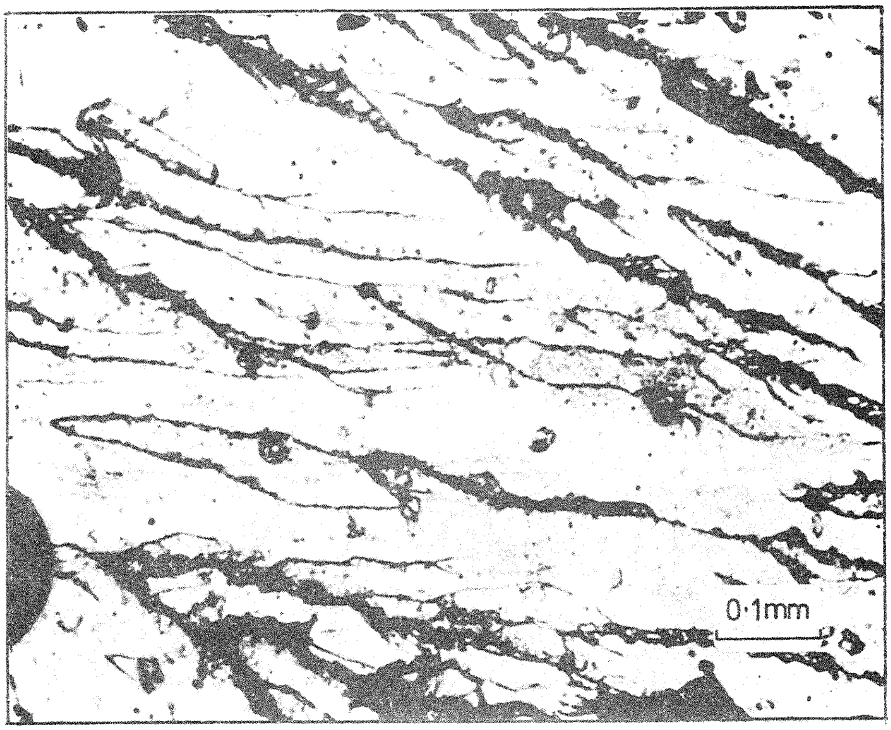

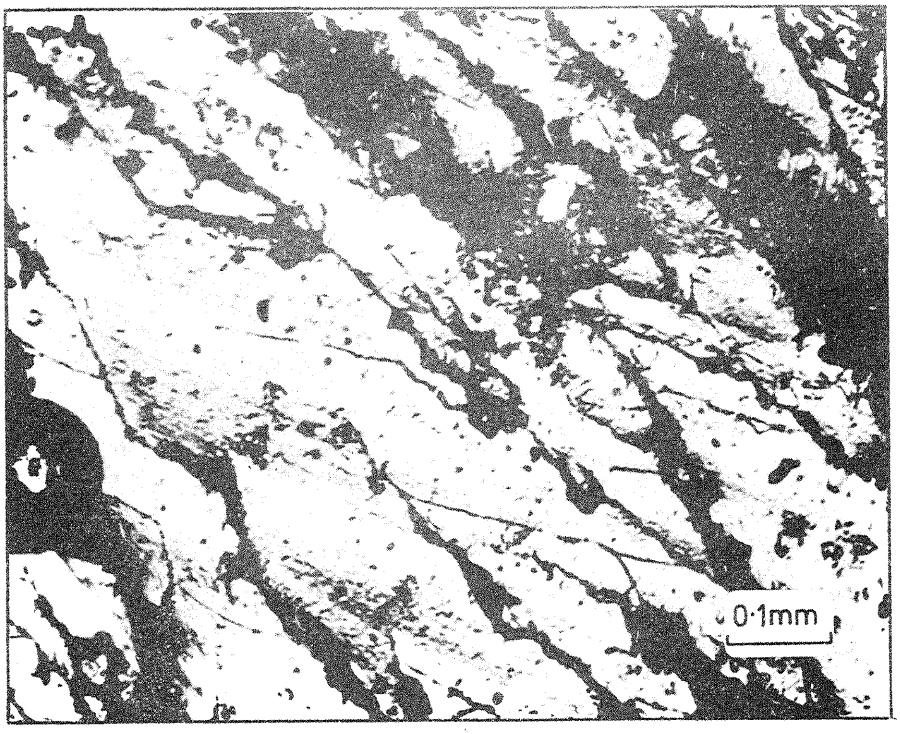

FIGURES 11, 12
STEP MARKINGS AND FINE DETAIL OF FRACTURE SURFACE

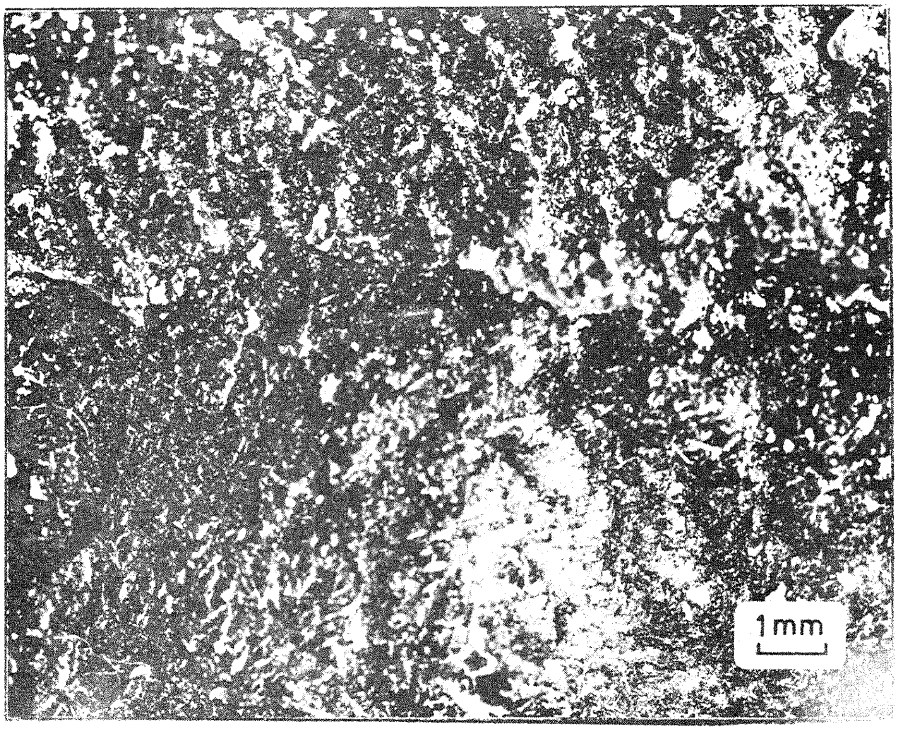

FIGURE 13
SURFACE OF SECONDARY FRACTURE. x10